Multi-Cancer Computational Analysis Reveals Metastasis-Associated Variant of Desmoplastic Reaction Involving INHBA and THBS2

Hoon Kim[1], John Watkinson[1], Vinay Varadan[2] and Dimitris Anastassiou[1*]

1 Center for Computational Biology and Bioinformatics and Department of Electrical Engineering, Columbia University, New York, NY, USA, **2** Philips Research North America, Briarcliff Manor, NY, USA

* Email: anastas@ee.columbia.edu

Abstract

Despite extensive research, the details of the metastasis-associated biological mechanisms are largely unknown. Here, we analyze data from multiple cancers using a novel computational method identifying sets of genes whose coordinated overexpression indicates the presence of a particular phenotype. We conclude that there is one shared "core" metastasis-associated gene expression signature corresponding to a specific variant of desmoplastic reaction, present in a large subset of samples that have exceeded a threshold of invasive transition specific to each cancer, indicating that the biological mechanism is triggered at that point. For example this threshold is reached at stage IIIc in ovarian cancer and at stage II in colorectal cancer. It has several features, such as coordinated expression of particular collagens, mainly *COL11A1* and other genes, mainly *THBS2* and *INHBA*. The universally prominent presence of INHBA in all cancers strongly suggests a biological mechanism centered on activin A induced TGF-β signaling, because activin A is a member of the TGF-β superfamily consisting of an INHBA homodimer. It is accompanied by the expression of several transcription factors related to epithelial-mesenchymal transition, but not of *SNAI1*, and expression of E-cadherin is not downregulated. It is reversible, as evidenced by its absence in many matched metastasized samples, but its presence indicates that metastasis has occurred. Therefore, these results can be used for developing high-specificity biomarkers, as well as potential multi-cancer metastasis-inhibiting therapeutics targeting the corresponding biological mechanism.

Introduction

It has been hypothesized [1,2] that the activation of some form of epithelial-mesenchymal transition (EMT) is a critical mechanism for the acquisition of motility and invasiveness in epithelial cancers. The version of EMT associated with cancer progression and metastasis has recently been labeled "Type 3 EMT" [2]. The details of the mechanisms have remained unclear, but it is believed that it involves activated fibroblasts in the desmoplastic stroma of tumors, referred to as "carcinoma associated fibroblasts" (CAFs), activation of some type of TGF-β signaling and significant involvement of the tumor microenvironment [3]. There is currently great interest in identifying the precise metastasis-associated features of type 3 EMT.

A study [4] of serous papillary ovarian carcinomas, comparing the gene expression profiles of primary vs. omental metastatic tumors, identified 156 differentially expressed genes. To investigate the significance of these genes in an independent rich data set we performed hierarchical clustering, using only these genes, on The Cancer Genome Atlas (TCGA) gene expression data set consisting of 377 ovarian cancer samples containing staging information. The resulting heat map revealed a prominent block of about 100 highly overexpressed genes in 94 samples (Figure S1, shown in www.ee.columbia.edu/~anastas/Figure_S1.pdf). Remarkably, we found that none of the 41 samples from tumors of stages IIIb and below were among the 94 samples. This cannot be due to chance ($P = 4 \times 10^{-6}$), leading to the hypothesis that coordinated overexpression of these genes implies that the tumour has metastasized into at least stage IIIc.

To further validate this hypothesis and test if similar versions apply to other cancers, we developed a computational technique (see Materials and Methods), which identifies, in an unbiased manner, clusters of coordinatedly overexpressed genes associated with a phenotype (such as transition to a particular metastatic stage). Our results consistently rediscover the same "core" signature of overexpressed genes, confirming the hypothesis. We found that this phenomenon occurs in multiple cancers, each of which has its own features involving additional genes, but the core signature is common. This common signature points to one particular variant of metastasis-associated desmoplastic reaction and to a corresponding particular variant of carcinoma associated fibroblasts to which we refer as "metastasis associated fibroblasts" (MAFs). Accordingly, in the following we refer to the corresponding gene expression signature and biological mechanism as "the MAF signature" and "the MAF mechanism," respectively.

Results

Since we focus on the cluster of genes associated with the metastasis binary ("low stage" versus "high stage") phenotype when the genes have their extreme (in most cases, largest) values, but not otherwise, we developed a special measure of association between the gene and the phenotype, which we call "extreme value association" (EVA), described in Materials and Methods. We performed the above algorithm on four rich gene expression data sets, two from ovarian cancer, the one from TCGA and another one [5], and two from colorectal cancer [6,7] accompanied by staging information. Using various staging transitions, it became clear that, in all cases, the MAF threshold can only be defined as exceeding stage IIIb in each of the ovarian data sets and stage I in each of the colorectal data sets. Interestingly, the "metastasis-associated

genes" identified in [4] as present in omental metastasis of ovarian cancer were also largely identified in [5] as belonging to a subtype of ovarian cancer characterized by extensive desmoplasia, which contains the MAF signature.

Remarkably, we found that there were many genes, each of which had Bonferroni-corrected $P < 10^{-3}$ in *all* four data sets. Table 1 shows a list of these genes with average log fold change greater than 2. The top ranked gene was *COL11A1* (probe 37892_at), followed by *COL10A1*, *POSTN*, *ASPN*, *THBS2*, and *FAP*. Again, these genes were found purely as a result of their association with the staging phenotype in all four cancers. Gene Ontology enrichment testing of these genes identified cell adhesion, extracellular matrix and collagen fibril organization.

We then did an extensive literature search aimed at identifying other studies in which at least some of these genes were identified as differentially expressed in various stages of other cancers. We even scrutinized studies in which none of the genes were mentioned in the main text, by looking at their supplementary data and re-ranking particular columns of genes in terms of their fold changes, from genes containing numerous genes. Although most of our results were negative, we were able to produce cancer gene lists with striking similarity (Table 2) to our own list (Table 1) in three studies of breast [8], gastric [9] and pancreatic [10] cancer.

Specifically, a breast cancer study [8] comparing ductal carcinomas in situ (DCIS) with invasive ductal carcinoma (IDC) had a list of genes upregulated in IDC (Table 2) that had similarities to those we had identified, and the top-ranked gene was again *COL11A1* (probe 37892_at) with log fold change of 6.50, while the next highest (4.08) corresponded to another probe of *COL11A1*, followed by a probe of *COL10A1*. Second, a study [9] comparing early gastric cancer (EGC) with advanced gastric cancer (AGC) – roughly separating stages I and II – also identified a similar differentially expressed gene list (Table 2) of which again *COL11A1* (probe 37892_at) was at the top (log fold change: 4.26) followed by *COL10A1* and *FAP*. Third, a study of pancreatic ductal adenocarcinoma [10] identified a list (Table 2) of gene overexpressed in whole tumor tissue versus normal pancreatic tissue, in which *COL11A1* (probe 37892_at) is again prominent and the top entry (log fold change 5.15) was *INHBA*, supportive of our hypothesis of activin induced TGF-β signaling. The presence of the MAF signature in the latter study indicates that pancreatic cancer had reached the MAF staging threshold in most cases before the biopsy. The prominent desmoplastic reaction in pancreatic cancers (which contains the MAF signature) has recently been increasingly recognized as a "foe" [11] that could lead to new therapeutic strategies targeting stromal cells to inhibit cancer. Finally, we realized that *COL11A1* has been identified as a potential metastasis-associated gene in other types of cancer as well, such as in lung [12], and oral cavity [13], suggesting that the MAF signature may be present in a subset of high stage samples of most if not all epithelial cancers.

In those cases as well as in our own findings, there was prominent presence of *COL11A1* (probe 37892_at). This remarkable consistent strong association of COL11A1 with the staging phenotype (specific to each cancer type) suggests that it could be used as a "proxy" of the MAF signature. This, in turn, allowed us to improve on the gene list of Table 1 by making use of numerous publicly available gene expression data sets of cancers of many types, even without any staging information, as long as the MAF signature is present in a sizeable subset of them, aiming at finding the "intersection" of the associated factors in these sets, revealing the "core" of the MAF biological mechanism.

As a first step for this task, we identified the few genes that are consistently highest associated with *COL11A1*. Table 3 shows a listing of genes in 22 cancer data sets, as well as an aggregate list of genes ranked in terms of their association with *COL11A1*. The list is very similar to the phenotype-based gene ranking (Table 1). In addition to *COL10A1* and a few other collagens, the top ranked genes are thrombospondin-2 (*THBS2*), inhibin beta A (*INHBA*), fibroblast activation protein (*FAP*), leucine rich repeat containing 15 (*LRRC15*), periostin (*POSTN*), and a disintegrin and metalloproteinase domain-containing protein 12 (*ADAM12*). The presence of FAP indicates a general desmoplastic reaction and is not, by itself, sufficient for inferring the MAF signature. Indeed, FAP is occasionally co-expressed with several other EMT-related genes even in healthy tissues. However, COL11A1 was *not* associated with any of these genes in neither healthy nor low-stage cancerous tissues, further supporting the hypothesis that it can be used as a proxy for the MAF signature. These results indicate that THBS2 and INHBA, top ranked in Table 3 except for collagens, are the most important players in the MAF mechanism.

As a second step, we identified gene pairs that are highest associated with COL11A1 jointly, but not individually, and therefore they would not appear in the previous list. For this task we ranked gene pairs according to their synergy [14] with COL11A1, using the computational method in [15], which could further facilitate biological discovery. For example, the scatter plots in Figure 1 show that genes *ECM2* and *TCF21* are jointly, but not individually, strongly associated with *COL11A1* ($P < 10^{-6}$, see Materials and Methods) in the two ovarian cancer data sets. Such findings are useful for developing biological hypotheses, e.g. in this particular case they suggest that the extracellular matrix protein 2 is associated with the MAF signature only when the *TCF21* gene (a known mesenchymal-epithelial transition mediator) is downregulated.

We only had miRNA and methylation data available for the TCGA ovarian data set. Using as measure the mutual information with *COL11A1*, we found many statistically significant miRNAs, among them hsa-miR-22 and hsa-miR-152, as well as differentially methylated genes, such as *SNAI1* and *PRAME*, suggesting a particularly complex biological mechanism (correlation with the MAF phenotype led to essentially the same lists with lower significance). Table 4 contains a list of the miRNAs, while Table 5 contains a list of the methylated genes (multiple test corrected $P < 10^{-16}$ in both cases, see Materials and Methods). *SNAI1* (*snail*) methylation is particularly important as the gene is known as one of the most important EMT-related transcription factors. Instead, the strongest MAF-associated transcription factor is AEBP1, making it a particularly interesting potential target. Many of the other EMT-related transcription factors, such as SNAI2, TWIST1, and ZEB1 are often overexpressed in the MAF signature, but SNAI1 is not (and, at least in ovarian carcinoma in which we have methylation data, this is due to its differentially methylated status). We believe that the lack of SNAI1 expression is a key distinguishing feature of the MAF signature, in which we observed neither SNAI1 overexpression nor CDH1 (E-cadherin) downregulation.

Discussion

A direct clinical application of these findings is the development of a high-specificity metastasis-sensing biomarker product detecting coordinated overexpression of a few top-ranked genes, such as *THBS2*, *INHBA* and the collagens *COL11A1*, *COL10A.* A positive result in

seemingly low-stage primary tumors will indicate that the disease has actually already reached a higher stage.

Remarkably, the same product can also be used to predict drug response. Indeed, at least in breast cancer, the MAF signature is associated with resistance to neoadjuvant chemotherapy. This is demonstrated in [16] where a stromal "metagene" signature of 50 genes was defined based on *DCN* (decorin). Although some of our key genes (such as *COL11A1*, *THBS2*) were not among these 50, the metagene signature used in that study has a strong intersection with the MAF signature. The stromal signature was resistant to neoadjuvant chemotherapy.

Of course, the most significant clinical application would be to develop metastasis-inhibiting therapeutics using targets deduced from the biological knowledge provided by the MAF signature. Our top ranked genes strongly suggest that a key feature of the MAF signature is fibroblast activation based on an activin A induced version of TGF-β signaling resulting in partial EMT lacking *SNAI1* expression, and leading to some form of altered proteolysis [17], which results in an environment rich in particular collagens, mainly COL11A1 and COL10A1. Supporting this hypothesis are the facts that activin A (INHBA homodimer) is a TGF-β superfamily member (ligand), THBS2 inhibits activation of TGF-β by THBS1, POSTN is highly homologous to the TGF-β induced gene *TGFBI*, and ADAM12 is known to have both protease activity and to contribute to TGF-β signaling [18]. The role of gene *LRRC15* (aka *LIB*) appears important but unclear, though it has already been recognized as promoting migration through the extracellular matrix [19] . Other related genes often present in the MAF signature that appear to be significant players in the mechanism are tissue inhibitor of metalloproteinases-3 (*TIMP3*), stromelysin-3 (*MMP11*), and cadherin-11 (*CDH11*). Overexpression of *INHBA* has been known to occur in cancers, occasionally accompanied by concomitant overexpression of the activin A receptors [20]. In one of the ovarian cancer data sets [5] we found that the MAF signature was accompanied ($P < 10^{-5}$) by concomitant overexpression of genes ACVRL1 aka ALK1 (Activin A type "II-like" 1 receptor, ACVR1 aka ALK2 (Activin A Type 1 receptor), and ACVR2A (Activin A Type 2A receptor). *ACVRL1* also consistently appears overexpressed and associated with INHBA expression in all cancers, suggesting that it plays a key role in the corresponding signaling mechanism. Remarkably, activin A is already known to facilitate fibroblast-mediated collagen gel contraction [21].

Although each of the MAF signature molecules could serve as a potential therapeutic target, alone or in combination, including miRNAs and methylated genes such as *SNAI1*, the hypothesis that activin A induced TGF-β signaling is at the heart of the MAF mechanism immediately suggests that follistatin (activin-binding protein) could serve as a metastasis inhibitor, which is exactly what recent research [22] indicates. Specifically, lung cancer cell lines transfected with follistatin and injected intravenously into immunodeficient mice markedly inhibited metastasis compared with non-transfected cell lines, but the authors of the study recognize that the role of follistatin in cancer metastasis is totally unknown [23]. Our work provides an explanation and suggests that the same could be true for other cancers as well. Further support is provided by the fact that follistatin virtually abolished the fibroblast–mediated collagen gel contraction mentioned earlier [21].

There are several reasons that the core MAF signature has not yet been discovered as a multi-cancer metastasis-associated signature. First, it is essential to define a precise phenotypic threshold recognizing that the signature only exists in a subset of tumors that exceed a particular

stage. Indeed, if the threshold in breast cancer was put between stage I and stage II, or between stage II and stage III, rather than between *in situ* and stage I, the signature would not be apparent, or it could even be reversed (see below). Second, each cancer type has its own additional features accompanying the MAF signature. For example, in ovarian cancer it is accompanied by sharp downregulation of genes *COLEC11*, *PEG3* and *TSPAN8*, which is not the case in other cancers. Indeed, the main contribution of our work is the identification of the common multi-cancer "core" signature, from which a universal metastasis-associated biological mechanism can be identified. Third and most importantly, the MAF signature is sharply reversible through a mesenchymal-epithelial transition (MET). For example [24], in a comparison of metastatic lymph node samples with their corresponding matched primary breast cancer samples, it was found that *COL11A1* had a much higher expression in the *primary* tumor samples. Such reverse results can be particularly confusing.

In fact, there are occasions in which the presence of the MAF signature in high-stage tumor samples (not having yet being reversed) can be an indicator of better prognosis, because many of the top-ranked genes in the MAF signature (such as thrombospondins, decorin, INHBA itself) are known to be potent anti-angiogenesis mediators. The reversal of the MAF signature would thus facilitate angiogenesis and further metastatic dissemination to distant sites. In other words, (a) the desmoplastic MAF signature and (b) angiogenesis, are two independent biological events. The former appears to based on activin A – induced TGF-β signaling (note that the same proteins mentioned above: thrombospondins, decorin, INHBA, etc, are also known inhibitors of the "standard" TGF-β ligand such as TGFB1. So, the reversal of the MAF signature would allow the standard ligand to take over in TGF beta signaling, and may thus facilitate angiogenesis. These observations provide explanations for the seemingly contradictory observed roles of TGF-β signaling in cancer and metastasis.

The reversibility of the MAF signature leads to the intriguing hypothesis that it is part of a dynamic process and perhaps all metastases have, at some point temporarily been there, which explains why we only observe it in a subset of them. It has already been recognized that "it is plausible, though hardly proven, that all types of carcinoma cells must undergo a partial or complete EMT to become motile and invasive [25] p. 600." This would be particularly exciting, because any metastasis-inhibiting therapeutic intervention targeting the MAF mechanism would be widely applicable to low-stage tumors.

In conclusion, we have shown that, using computational analysis of publicly available biological information, systems biology has revealed the core of a multi-cancer metastasis-associated gene expression signature. In the near future, a vast amount of additional information will become available, including next generation sequencing, miRNA and methylation information for many cancers, which will allow additional computational research building on this work and clarifying the details of the underlying complex biological process.

Materials and Methods

The gene expression data sets used in this paper are described in Table 6.

Extreme Value Association (EVA)

The EVA metric is the minimum *P* value of biased partitions over all subsets of samples with highest expression values of the gene. In other words, suppose that there are totally *M* samples, out of which *N* are "low stage" and *M* – *N* are "high stage," and we select the *m* samples with the highest gene expression values. Under the assumption that gene expression values are uncorrelated with the phenotype, the probability that there will be at most *n* "low stage" samples among the selected *m* samples is given by the cumulative hypergeometric probability $h(x \le n; M, N, m)$. The EVA metric is then equal to $-\log_{10}$ of the minimum of these probabilities over all possible values of *n*. For example, assume that there are 250 high-stage samples and 50 low-stage sample for a total of 300 samples. Furthermore, assume that the 100 samples with the highest values of a particular gene contain 99 high-stage samples and one low-stage sample. In that case, $h(x \le 1; 300, 50, 100)$ can be evaluated using the MATLAB function hypercdf(1,300,50,100) = 5×10^{-9}, resulting in the EVA metric for that gene of *at least* $-\log_{10}(5\times10^{-9}) = 8.3$, e.g. if the 101th sample is also high-stage, then the EVA metric of the gene will be even higher. Note that, once the highest value is reached, the sorting arrangement of the remaining samples is irrelevant, reflecting the hypothesis that only the extreme values are associated with the phenotype. Figure 2 shows the values of the cumulative hypergeometric probability for the *COL11A1* gene using the TCGA ovarian cancer data set and the staging threshold between IIIb and IIIc: The maximum (8.31) occurs when *m* = 133. In fact, all 133 samples with the highest *COL11A1* expression are at stage IIIc or IV.

We then developed a mechanistic unbiased (only dependent on the phenotype) algorithm, which, when given a gene expression data set for a number of samples labelled "high stage" or "low stage," leads to a selection of genes that are coordinatedly overexpressed only in high-stage samples. We first select the top 100 genes that rank highest according to the EVA metric criterion. Using this set of genes only, we perform k-means clustering with gap statistic [26]. At that step, if indeed the genes are coordinately overexpressed, they will align well in the heat map. This leads to the selection of the samples belonging to the cluster most associated with the high/low stage phenotype – call this the set of "EVA-based samples." Nearly all samples in that cluster have exceeded the MAF staging threshold, and the very few exceptions could be due to misdiagnosis. Next, we define a "clean" MAF phenotype, contrasting the samples that are: (a) both "EVA-based" and "high-stage" against (b) the samples that are both "non EVA-based" and "low stage." If the number of samples is sufficiently large, this "clean" phenotype provides the sharpest way by which we can identify the genes that are most associated with the observed phenomenon of metastasis-associated coordinated overexpression. We then rank the genes and compute their multiple-test-corrected *P* values using a heteroscedastic t-test using the "clean" phenotype and select the genes for which $P < 10^{-3}$ after Bonferroni correction. Finally, we find the intersection of these selected gene sets over all cancer expression data sets and rank them in terms of fold change.

For a data set with *n* samples and *m* probe sets, The EVA algorithm computes $n \times m$ cumulative hypergeometric distribution probabilities. This can be quite computationally intensive, so we

devised a low-complexity implementation algorithm to dynamically "build" the cumulative hypergeometric distribution for each probe set as the EVA algorithm progresses, as follows:

Given a data set with *a* high-stage samples and *b*-low stage samples, the idea is to construct an $(a+1)\times(b+1)$ table of the hypergeometric probabilities corresponding to all possible subsets of the samples. Then, for each probe set, the samples are sorted according to the expression value of the probe set. This ordering results in a path through the table from the bottom left corner to the top right corner, moving either up or to the right for each sample. At each step in the path, the cumulative probability of encountering the observed number of high stage samples or more is computed by summing the entries diagonally down and to the right of the current cell, including the current cell itself. The algorithm is best demonstrated with a visual example shown in Figure 3, in which the data set has three low stage samples and five high stage samples in total. Each probe set results in a path through this table, and an example path is displayed here in gray. Letting *1* correspond to a high stage sample and *0* correspond to a low stage sample, this example probe set results in the path *111001011*. For the cell in blue, corresponding to the sub-path *111001*, the probability of encountering this many high stage samples or more is computed by summing the three probabilities diagonally down and to the right of the blue cell (including itself). In this case, the probability is quite high (82.2%). This cumulative probability is computed for every step along the path, and the minimum of these is the output of the EVA algorithm.

The pseudo-code for this algorithm is given below:

```
Input:
Let n be the number of samples.
Let a be the number of high stage samples.
Let b be the number of low stage samples.
Let s be the array of phenotype labels sorted by this probe set's expression level
(Note: a + b = n)

Algorithm:
// Step 1 – Build the table of hypergeometric probabilities.
// This step need only be run once for the entire data set.
Define c as an array with (a+1) rows and (b+1) columns.
For x from 0 to a
  For y from 0 to b
    If x = 0 and y = 0
       c[x][y] = 0
    Else
       If (y > 0)
         c[x][y] = c[x][y] + c[x][y - 1] * (b - y + 1) / ((b - y + 1) + (a - x))
       End if
       If (x > 0)
         c[x][y] = c[x][y] + c[x - 1][y] * (a - x + 1) / ((a - x + 1) + (b - y))
       End If
    End If
  End For
End For
// Step 2 – Compute the cumulative hypergeometric probability for the given sequence.
Define x = 0
Define y = 0
Define bestP = 1
For i from 1 to n
  If (s[i] = 1)
    x = x + 1
  Else
    y = y + 1
```

```
  End If
  Define p = 0
  For j from 0 to y
    If (x + y - j <= a)
      p = p + c[x + y - j][j]
    End If
  End For
  If (p < bestP)
    bestP = p
  End If
End For

Output:
  -log10(bestP)
```

Mutual Information and Synergy

Assuming that two variables, such as the expression levels of two genes G_1 and, G_2 are governed by a joint probability density p_{12} with corresponding marginals p_1 and p_2 and using simplified notation, the mutual information $I(G_1;G_2)$ is a general measure of correlation and is defined as the expected value $E\left\{\log\frac{p_{12}}{p_1 p_2}\right\}$. The synergy of two variables G_1, G_2 with respect to a third variable G_3 is [14] equal to $I(G_1,G_2;G_3)-\left[I(G_1;G_3)+I(G_2;G_3)\right]$, i.e., the part of the association of the pair G_1, G_2 with G_3 that is purely due to a synergistic cooperation between G_1 and G_2 (the "whole" minus the sum of the "parts").

P value evaluation for the significance of miRNA and methylation sites, and for synergistic pair *ECM2* and *TCF21*

We applied a permutation-based approach accounting for multiple test correction: We did 100 permutation experiments of the class labels, saving the corresponding 100 highest values after doing exhaustive search in each permutation experiment. Using the set of these 100 highest-value scores, we obtained the maximum likelihood estimates of the location parameter and the scale parameter of the Gumbel (type-I extreme value) distribution, resulting in a cumulative density function F. The *P* value of an actual score x_0 is then 1-F(x_0) under the null hypothesis of no association with phenotype. Similarly, for the synergistic pair, we found the top-scoring synergy in 100 data sets that were identical to the original except that the COL11A1 probe values were randomly permuted on each, and the top permuted synergy scores were modelled, as above, with the Gumbel distribution.

References

1. Thiery JP (2002) Epithelial-mesenchymal transitions in tumour progression. Nat Rev Cancer 2: 442-454.
2. Kalluri R, Weinberg RA (2009) The basics of epithelial-mesenchymal transition. J Clin Invest 119: 1420-1428.
3. Stover DG, Bierie B, Moses HL (2007) A delicate balance: TGF-beta and the tumor microenvironment. J Cell Biochem 101: 851-861.
4. Bignotti E, Tassi RA, Calza S, Ravaggi A, Bandiera E, et al. (2007) Gene expression profile of ovarian serous papillary carcinomas: identification of metastasis-associated genes. Am J Obstet Gynecol 196: 245 e241-211.
5. Tothill RW, Tinker AV, George J, Brown R, Fox SB, et al. (2008) Novel molecular subtypes of serous and endometrioid ovarian cancer linked to clinical outcome. Clin Cancer Res 14: 5198-5208.
6. Jorissen RN, Gibbs P, Christie M, Prakash S, Lipton L, et al. (2009) Metastasis-Associated Gene Expression Changes Predict Poor Outcomes in Patients with Dukes Stage B and C Colorectal Cancer. Clin Cancer Res 15: 7642-7651.
7. Smith JJ, Deane NG, Wu F, Merchant NB, Zhang B, et al. Experimentally derived metastasis gene expression profile predicts recurrence and death in patients with colon cancer. Gastroenterology 138: 958-968.
8. Schuetz CS, Bonin M, Clare SE, Nieselt K, Sotlar K, et al. (2006) Progression-specific genes identified by expression profiling of matched ductal carcinomas in situ and invasive breast tumors, combining laser capture microdissection and oligonucleotide microarray analysis. Cancer Res 66: 5278-5286.
9. Vecchi M, Nuciforo P, Romagnoli S, Confalonieri S, Pellegrini C, et al. (2007) Gene expression analysis of early and advanced gastric cancers. Oncogene 26: 4284-4294.
10. Badea L, Herlea V, Dima SO, Dumitrascu T, Popescu I (2008) Combined gene expression analysis of whole-tissue and microdissected pancreatic ductal adenocarcinoma identifies genes specifically overexpressed in tumor epithelia. Hepatogastroenterology 55: 2016-2027.
11. Apte MV, Wilson JS (2007) The Desmoplastic Reaction in Pancreatic Cancer: An Increasingly Recognised Foe. Pancreatology 7: 378-379.
12. Chong IW, Chang MY, Chang HC, Yu YP, Sheu CC, et al. (2006) Great potential of a panel of multiple hMTH1, SPD, ITGA11 and COL11A1 markers for diagnosis of patients with non-small cell lung cancer. Oncol Rep 16: 981-988.
13. Schmalbach CE, Chepeha DB, Giordano TJ, Rubin MA, Teknos TN, et al. (2004) Molecular profiling and the identification of genes associated with metastatic oral cavity/pharynx squamous cell carcinoma. Arch Otolaryngol Head Neck Surg 130: 295-302.
14. Anastassiou D (2007) Computational analysis of the synergy among multiple interacting genes. Mol Syst Biol 3: 83.
15. Watkinson J, Liang KC, Wang X, Zheng T, Anastassiou D (2009) Inference of regulatory gene interactions from expression data using three-way mutual information. Ann N Y Acad Sci 1158: 302-313.

16. Farmer P, Bonnefoi H, Anderle P, Cameron D, Wirapati P, et al. (2009) A stroma-related gene signature predicts resistance to neoadjuvant chemotherapy in breast cancer. Nat Med 15: 68-74.
17. Kessenbrock K, Plaks V, Werb Z (2010) Matrix metalloproteinases: Regulators of the tumor microenvironment. Cell 141: 52-67.
18. Atfi A, Dumont E, Colland F, Bonnier D, L'Helgoualc'h A, et al. (2007) The disintegrin and metalloproteinase ADAM12 contributes to TGF-beta signaling through interaction with the type II receptor. J Cell Biol 178: 201-208.
19. Satoh K, Hata M, Shimizu T, Yokota H, Akatsu H, et al. (2005) Lib, transcriptionally induced in senile plaque-associated astrocytes, promotes glial migration through extracellular matrix. Biochem Biophys Res Commun 335: 631-636.
20. Kleeff J, Ishiwata T, Friess H, Buchler MW, Korc M (1998) Concomitant over-expression of activin/inhibin beta subunits and their receptors in human pancreatic cancer. Int J Cancer 77: 860-868.
21. Ohga E, Matsuse T, Teramoto S, Ouchi Y (2000) Activin receptors are expressed on human lung fibroblast and activin A facilitates fibroblast-mediated collagen gel contraction. Life Sci 66: 1603-1613.
22. Talmadge JE (2008) Follistatin as an inhibitor of experimental metastasis. Clin Cancer Res 14: 624-626.
23. Ogino H, Yano S, Kakiuchi S, Muguruma H, Ikuta K, et al. (2008) Follistatin suppresses the production of experimental multiple-organ metastasis by small cell lung cancer cells in natural killer cell-depleted SCID mice. Clin Cancer Res 14: 660-667.
24. Ellsworth RE, Seebach J, Field LA, Heckman C, Kane J, et al. (2009) A gene expression signature that defines breast cancer metastases. Clin Exp Metastasis 26: 205-213.
25. Weinberg RA (2007) The biology of cancer. New York: Garland Science. 1 v. (various pagings) p.
26. Tibshirani R, Walther G, Hastie T (2001) Estimating the number of clusters in a dataset via the Gap statistic. J R Statist Soc B 63: 411-423.

Figure Legends and Figures

Figure 1: Example of a synergistic pair of genes in two ovarian cancer datasets

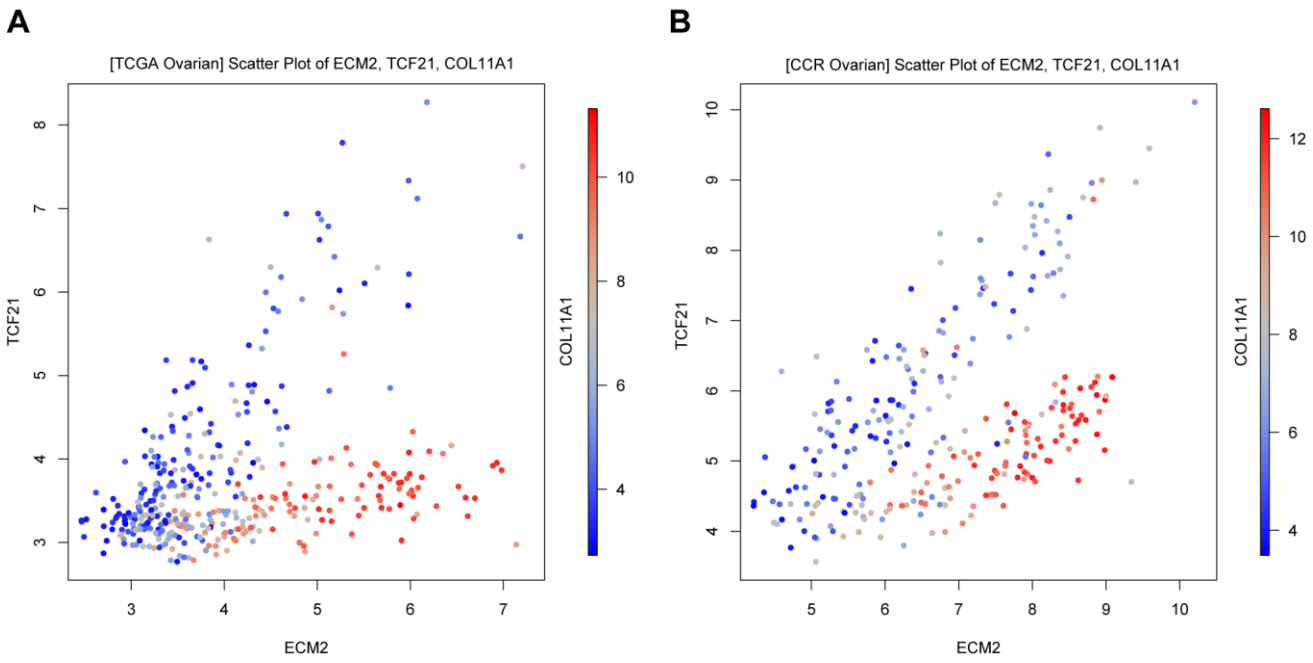

Figure 2: Evaluation of the EVA metric for gene *COL11A1* in the TCGA ovarian cancer dataset using phenotypic staging threshold the transition to stage IIIc.

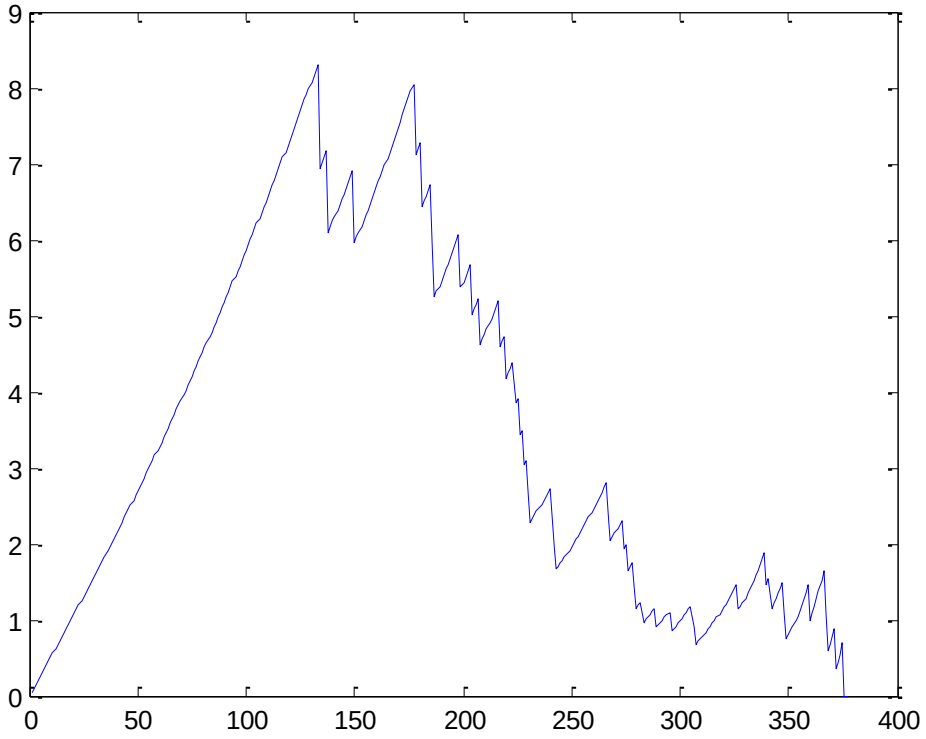

Figure 3: Illustration for the low-complexity implementation of the EVA algorithm.

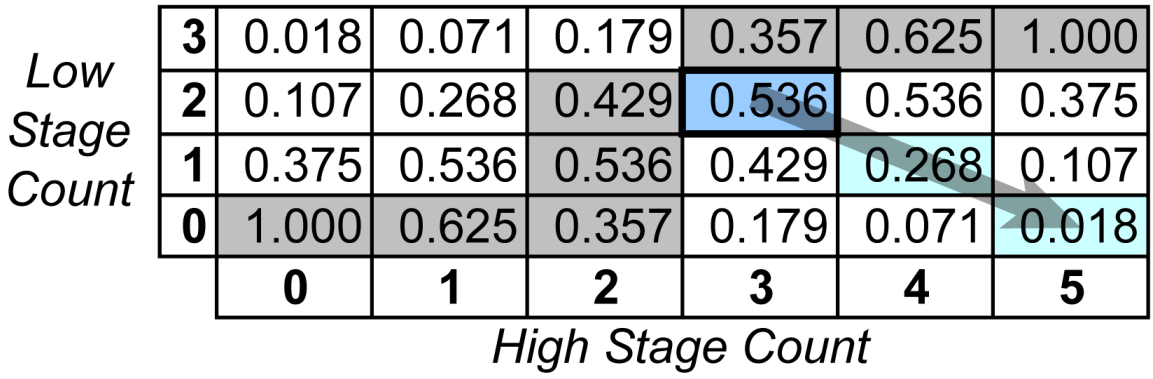

Tables

Table 1: Top-ranked genes associated with high carcinoma stage in ovarian and colorectal cancers according to the EVA-based algorithm with Bonferroni corrected $P < 10^{-3}$ in all four data sets

Probe Set[a]	Gene	Log FC
37892_at	COL11A1	3.94
217428_s_at	COL10A1	3.55
204320_at	COL11A1	3.39
210809_s_at	POSTN	3.14
219087_at	ASPN	2.99
205941_s_at	COL10A1	2.88
203083_at	THBS2	2.81
209955_s_at	FAP	2.73
215446_s_at	LOX	2.63
213764_s_at	MFAP5	2.61
210511_s_at	INHBA	2.52
215646_s_at	VCAN	2.5
209758_s_at	MFAP5	2.42
221730_at	COL5A2	2.34
211571_s_at	VCAN	2.33
205713_s_at	COMP	2.31
213765_at	MFAP5	2.27
201150_s_at	TIMP3	2.25
221729_at	COL5A2	2.24
212354_at	SULF1	2.23
212489_at	COL5A1	2.22
213790_at	ADAM12	2.21
212488_at	COL5A1	2.2
201147_s_at	TIMP3	2.19
204457_s_at	GAS1	2.17
202952_s_at	ADAM12	2.12
202766_s_at	FBN1	2.08
212344_at	SULF1	2.07

[a]Affymetrix probe sets

Table 2: Gene lists produced from information provided in the corresponding papers for breast, gastric and pancreatic cancer.

Breast Cancer, Shuetz et al[a]			Gastric cancer, Vecchi et al[b]			Pancreatic cancer, Badea et al[c]		
Probe Set[d]	Gene Symbol	Log FC	Probe Set[d]	Gene Symbol	Log FC	Probe Set[d]	Gene Symbol	Log FC
37892_at	*COL11A1*	6.50	37892_at	*COL11A1*	4.26	227140_at	*INHBA*	5.15
204320_at	*COL11A1*	4.08	217428_s_at	*COL10A1*	4.15	217428_s_at	*COL10A1*	5.00
217428_s_at	*COL10A1*	4.07	209955_s_at	*FAP*	3.40	1555778_a_at	*POSTN*	4.92
213764_s_at	*MFAP5*	3.73	235458_at	*HAVCR2*	3.30	212353_at	*SULF1*	4.63
213909_at	*LRRC15*	3.61	204320_at	*COL11A1*	3.28	226237_at	*COL8A1*	4.60
205941_s_at	*COL10A1*	3.52	205941_s_at	*COL10A1*	3.21	37892_at	*COL11A1*	4.40
210511_s_at	*INHBA*	3.44	204052_s_at	*SFRP4*	2.90	225681_at	*CTHRC1*	4.38
202766_s_at	*FBN1*	3.43	226930_at	*FNDC1*	2.85	202311_s_at	*COL1A1*	4.12
212353_at	*SULF1*	3.35	227140_at	*INHBA*	2.77	203083_at	*THBS2*	3.97
218468_s_at	*GREM1*	3.35	209875_s_at	*SPP1*	2.77	227566_at	*HNT*	3.90
215446_s_at	*LOX*	3.22	205422_s_at	*ITGBL1*	2.63	204619_s_at	*CSPG2*	3.87
221730_at	*COL5A2*	3.22	226311_at	---	2.63	229802_at	*WISP1*	3.80
218469_at	*GREM1*	3.20	222288_at	---	2.62	212464_s_at	*FN1*	3.69
212489_at	*COL5A1*	3.08	231993_at	---	2.50	205713_s_at	*COMP*	3.53
203083_at	*THBS2*	2.99	226237_at	*COL8A1*	2.48	221729_at	*COL5A2*	3.38
201505_at	*LAMB1*	2.97	223122_s_at	*SFRP2*	2.47	209955_s_at	*FAP*	3.37
209955_s_at	*FAP*	2.96	210511_s_at	*INHBA*	2.43	229218_at	*COL1A2*	3.16
209758_s_at	*MFAP5*	2.92	203819_s_at	*IMP-3*	2.39	209016_s_at	*KRT7*	3.13
202363_at	*SPOCK*	2.91	212464_s_at	*FN1*	2.36	210004_at	*OLR1*	3.03
213241_at	*NY-REN-58*	2.90	212353_at	*SULF1*	2.35	219773_at	*NOX4*	3.02
205479_s_at	*PLAU*	2.89	227995_at	---	2.34	218804_at	*TMEM16A*	2.90
206584_at	*LY96*	2.88	225681_at	*CTHRC1*	2.30	238617_at	---	2.87
204475_at	*MMP1*	2.83	204457_s_at	*GAS1*	2.27	224694_at	*ANTXR1*	2.82
202952_s_at	*ADAM12*	2.83	216442_x_at	*FN1*	2.25	228481_at	*COX7A1*	2.77
201792_at	*AEBP1*	2.81	223121_s_at	*SFRP2*	2.23	226311_at	*ADAMTS2*	2.76
204114_at	*NID2*	2.81	211719_x_at	*FN1*	2.23	201792_at	*AEBP1*	2.68
213790_at	*ADAM12*	2.80	204776_at	*THBS4*	2.18	203021_at	*SLPI*	2.65
209156_s_at	*COL6A2*	2.77	210495_x_at	*FN1*	2.15	227314_at	*ITGA2*	2.58
219179_at	*DACT1*	2.74	202800_at	*SLC1A3*	2.13	205499_at	*SRPX2*	2.44
212488_at	*COL5A1*	2.73	214927_at	---	2.11	226997_at	---	2.41
219087_at	*ASPN*	2.73	212354_at	*SULF1*	2.09	219179_at	*DACT1*	2.36
204619_s_at	*CSPG2*	2.70	238654_at	*LOC147645*	2.06	203570_at	*LOXL1*	2.30
204337_at	*RGS4*	2.69	213943_at	*TWIST1*	2.06	201850_at	*CAPG*	2.25
204620_s_at	*CSPG2*	2.69	236028_at	*IBSP*	2.05	222449_at	*TMEPAI*	2.19
212354_at	*SULF1*	2.68	228481_at	*POSTN*	2.00	227276_at	*PLXDC2*	2.16

[a]Breast cancer list indicates genes overexpressed in invasive ductal carcinoma vs. ductal carcinoma in situ.
[b]Gastric cancer list indicates genes overexpressed in early gastric cancer vs. advanced gastric cancer.
[c]Pancreatic cancer list indicates genes overexpressed in pancreatic ductal adenocarcinoma vs. normal pancreatic tissue.
[d]Affymetrix probe sets

Table 3: Genes associated with *COL11A1* from various cancers

						expO data sets															
TCGA OV	CCR OV	CCR Colon	Moffitt Colon	Singapore Gastric	Yu Multicancer Tumor	batch 1	batch 2	batch 3	batch 4	batch 5	batch 6	batch 7	batch 8	batch 9	batch 10	batch 11	batch 12	batch 13	batch 14	batch 15	batch 16
COL11A1	COL11A1	COL11A1	COL11A1	COL11A1	COL11A1	COL11A1	COL11A1	COL11A1	COL11A1	COL11A1	COL11A1	COL11A1	COL11A1	COL11A1	COL11A1	COL11A1	COL11A1	COL11A1	COL11A1	COL11A1	COL11A1
THBS2	FAP	COL10A1	COL10A1	COL10A1	COL10A1	COL10A1	COL10A1	COL10A1	COL10A1	COL10A1	COL10A1	COL10A1	COL10A1	COL10A1	COL10A1	COL10A1	COL1A1	COL10A1	COL10A1	COL10A1	COL1A1
COL5A2	POSTN	THBS2	ADAM12	MMP11	LRRC15	ADAM12	LRRC15	COL1A1	THBS2	LRRC15	CTHRC1	INHBA	LRRC15	COL1A1	COL1A1	ADAMTS12	COL10A1	LRRC15	LRRC15	ADAMTS12	ADAMTS12
INHBA	THBS2	ADAM12	HNT	COL1A1	COL1A2	ADAMTS12	MXRA5	CTHRC1	COL1A2	ADAM12	COL5A2	COL1A1	COL1A1	LRRC15	FNDC1	COL1A1	COL3A1	ADAMTS12	FNDC1	COL1A1	COL5A2
COL5A1	HNT	HNT	THBS2	ADAMTS12	MMP11	PPAPDC1A	ADAMTS12	COL5A2	FAP	COL1A1	LRRC15	ADAMTS12	THBS2	CTHRC1	LRRC15	COL5A2	COL12A1	COL1A1	ADAM12	COL3A1	CTHRC1
POSTN	INHBA	CTHRC1	RAB31	THBS2	COL1A1	COL12A1	PPAPDC1A	COL5A1	COL1A1	COL1A2	FAP	THBS2	INHBA	INHBA	ADAMTS12	INHBA	COL5A1	ADAM12	INHBA	LRRC15	COL5A1
VCAN	EPYC	SPOCK1	COL5A2	INHBA	COL5A2	CTHRC1	ADAM12	THBS2	INHBA	FAP	POSTN	CTHRC1	COMP	COL5A2	COL5A2	LRRC15	ADAMTS12	FN1	ADAMTS12	COL5A2	FNDC1
MMP11	COL5A2	BGN	CTHRC1	SULF1	INHBA	FNDC1	COL5A2	COL1A2	ADAMTS12	COL5A1	COL5A1	LRRC15	COL1A2	COL1A2	COL5A1	CTHRC1	FNDC1	COL1A2	FAP	COL5A1	COL1A2
FAP	COL10A1	FAP	SPOCK1	CTHRC1	COL5A1	THBS2	FNDC1	MXRA5	COL5A2	ADAMTS12	ADAMTS12	FNDC1	COL5A2	COL5A1	FAP	FAP	COL5A2	FNDC1	CTHRC1	ITGA11	LRRC15
LRRC15	LRRC15	INHBA	SULF1	PPAPDC1A	VCAN	PLAU	COL1A2	LRRC15	LRRC15	COL12A1	COL1A1	COL5A2	CTHRC1	FN1	CTHRC1	POSTN	FAP	COL5A1	COL5A2	MFAP5	COL3A1
COL3A1	SFRP2	PPAPDC1A	INHBA	WNT2	THBS2	ANTXR1	COL8A2	ADAMTS12	COL5A1	INHBA	THBS2	COL5A1	POSTN	FNDC1	POSTN	COL5A1	ADAM12	PLAU	COL1A1	FAP	INHBA
COL1A1	VCAN	SULF1	GAS1	COL5A2	COL3A1	COL5A2	COL5A1	FNDC1	POSTN	POSTN	COL3A1	COL3A1	COL5A1	THBS2	INHBA	COL3A1	COL1A2	EPYC	POSTN	COL1A2	FAM49B
CTSK	FN1	COL1A1	AEBP1	C5orf46	ADAM12	ITGA11	CTHRC1	POSTN	FNDC1	THBS2	COL1A2	POSTN	SFRP2	ADAMTS12	THBS2	THBS2	CTHRC1	COL5A2	THBS2	FNDC1	FAP
LOX	ADAMTS12	VCAN	SPARC	ANTXR1	BGN	FAP	FAP	FAP	ADAM12	COL3A1	INHBA	COL1A2	COL3A1	FAP	COL3A1	CTSK	MXRA5	COL3A1	COL3A1	PPAPDC1A	THBS2
LUM	LOX	COL5A2	FBN1	HNT	FAP	COL1A2	COMP	COL3A1	COL3A1	COL5A2	FNDC1	ITGA11	AEBP1	COL3A1	COL1A2	FNDC1	PLAU	PPAPDC1A	PPAPDC1A	INHBA	ADAM12
CRISPLD2	ALPK2	ADAMTS12	COL1A2	FN1	AEBP1	NOX4	SFRP2	AEBP1	FN1	COL8A2	COL12A1	FAP	MXRA5	POSTN	ADAM12	ADAM12	LRRC15	CTHRC1	COL5A1	POSTN	COL10A1
COL10A1	COL3A1	POSTN	COL5A1	FNDC1	MFAP5	COL5A1	THBS2	COMP	CTHRC1	CTHRC1	COL6A3	SFRP2	ADAMTS12	COL12A1	COL12A1	COL1A2	POSTN	FAP	TPX2	CTHRC1	PLAU
FBN1	GREM1	RAB31	PRRX1	SPHK1	CDH11	SULF1	COL3A1	FBN1	ITGA11	ITGA11	SFRP2	FN1	FAP	ITGBL1	COL6A3	TNFSF4	THBS2	FAM49B	FN1	MFAP2	PDPN
FN1	COL5A1	AEBP1	COL1A1	KAL1	SULF1	FN1	EPYC	COL6A3	PPAPDC1A	MXRA5	SULF1	PPAPDC1A	COL8A2	COMP	COMP	EPYC	EPYC	SULF1	SFRP2	ADAM12	GKAP1
ADAM12	ADAM12	COL1A2	MXRA5	COL1A2	COL6A3	SRPX2	MFAP5	FN1	AEBP1	CDH11	COMP	AEBP1	LOXL1	SFRP2	MXRA5	COL8A2	INHBA	INHBA	CDKN3	THBS2	POSTN
MMP2	COL1A1	PRRX1	FAP	NOX4	POSTN	COL1A1	COL1A1	COL8A2	SULF1	COL6A3	MXRA5	VCAN	ADAM12	COL8A2	CTSK	ITGBL1	CTSK	IGFL2	HGD	HTRA3	KIAA1199
AEBP1	CRISPLD2	COL5A1	BGN	CST1	MMP13	MXRA5	LOC401097	SPARC	HNT	FN1	ADAM12	SULF1	FNDC1	ITGA11	GLT8D2	MXRA5	PDPN	POSTN	UBE2C	ALDH1L2	MMP14
PLAU	MMP11	KAL1	POSTN	BGN	CTSK	EPYC	COL12A1	SFRP2	COL6A3	FNDC1	PRRX1	MXRA5	COL6A3	SULF1	ITGBL1	COL12A1	SFRP2	SLC12A8	COL1A2	RCN3	SRPX2
ASPN	PRRX1	SFRP4	SFRP2	SOX11	LUM	COL8A2	ANTXR1	INHBA	SPARC	COMP	AEBP1	CDH11	RCN3	SPARC	CDH11	COL6A3	MMP2	C15orf48	ASPM	ASPN	IGHG1
TMEM158	TMEM158	FBN1	PPAPDC1A	ITGA11	PPAP2B	WISP1	ITGA11	SULF1	FBN1	ASPN	COL16A1	ADAM12	SULF1	TIMP3	FN1	GREM1	SRPX2	THBS2	KIF4A	COL6A3	ADA
ECM1	CTSK	SFRP2	NOX4	CST4	FN1	THY1	RUNX2	VCAN	COL12A1	MFAP2	PPAPDC1A	COL12A1	MFAP5	GLT8D2	COL8A2	GLT8D2	SULF1	MXRA5	NUF2	ITGBL1	ADAM19
COL1A2	SPARC	ANTXR1	VCAN	COL5A1	RCN3	LRRC15	TNFSF4	PPAPDC1A	MXRA5	PPAPDC1A	MFAP2	COL6A3	VCAN	ADAM12	EPYC	PDPN	RCN3	EPHB2	CENPF	SRPX2	BMP1
SPARC	FBN1	GAS1	ANTXR1	FAP	TPO	IGFL2	COL6A3	COL12A1	VCAN	AEBP1	CTSK	COL8A2	LUM	CDH11	VCAN	SULF1	COL6A3	DLGAP5	ACADL	GREM1	SFRP2
EPYC	CTHRC1	COL3A1	FRMD6	MMP14	OLFML2B	CDH11	PDGFRL	DCN	COMP	MMP13	COL8A2	BGN	PCOLCE	MXRA5	SULF1	FN1	MMP1	KIF20A	PLAU	MXRA5	C11orf52
COL6A3	GJB2	FNDC1	COL3A1	LRRC15	KCNJ16	POSTN	ALDH1L2	CTSK	COL8A2	SFRP2	SERPINF1	HNT	COL12A1	RCN3	SPARC	COMP	PLAUR	MFAP5	DTL	FBN1	HPN
SERPINF1	TNFAIP6	HOPX	ADAMTS12	SERPINH1	MXRA5	COL3A1	GLT8D2	ITGBL1	WISP1	COL6A2	GLT8D2	SPARC	FN1	FBN1	DCN	CDH11	GREM1	CDC2	COL12A1	BMP1	TRAM2
OLFML2B	NUAK1	NOX4	TIMP2	POSTN	NNMT	HNT	CTSK	GLT8D2	GLT8D2	VCAN	CDH11	COMP	FBN1	AEBP1	LUM	WISP1	ALDH1L2	LIMK2	C2orf67	COL12A1	GJB2
DCN	ASPN	LOX	COL12A1	SPP1	PAX8	INHBA	FBN1	OLFML2B	MRC2	SULF1	PCOLCE	TNFSF4	MFAP2	VCAN	SFRP2	HNT	FBN1	MFAP2	RNF180	MRC2	ECHDC2
ACTA2	AEBP1	CERCAM	LOX	ADAM12	DUOX2	TNFSF4	TWIST1	ANTXR1	RCN3	ANTXR1	FN1	RCN3	PRRX1	HNT	PLAU	FBN1	MMP3	LOC401097	BIRC5	COMP	ELF4
NTM	COL8A1	COL12A1	HTRA1	CLEC5A	DCN	COL6A3	INHBA	TNFAIP6	ANTXR1	CTSK	HNT	GREM1	PLAU	COL8A1	HNT	ALDH1L2	CEACAM6	MMP11	CDC20	VCAN	CTSK
GREM1	COL1A2	SPARC	TWIST1	BMP1	TG	PDGFRL	FN1	MMP2	CTSK	PCOLCE	FBN1	EPYC	RAB31	LOX	IGHG1	RCN3	C11orf24	SLAMF8	CENPA	CERCAM	C3orf15
CDH11	LUM	BCAT1	BCAT1	CAPN6	TNFAIP6	MMP14	ZNF469	CCDC80	SFRP2	SPARC	DCN	SALL1	MMP11	CERCAM	FBN1	PLAU	NINJ2	LMNB1	LOC730057	COL8A2	TRIM59
SNAI2	TIMP3	ITGBL1	ISLR	VCAN	GPX3	SPARC	HNT	MRC2	ASPN	LOXL1	LUM	MFAP5	ISLR	BGN	RCN3	ASPN	PPAPDC1A	GTSE1	RRM2	CDH11	COL6A3
TIMP3	EDNRA	FRMD6	KAL1	ZNF469	LOX	RCN3	GAS1	PCOLCE	PRRX1	PRRX1	GAS1	LOX	CRABP2	THY1	MMP2	SFRP2	KIAA1199	ZWINT	CASC5	ISLR	FGFR1OP2
PDLIM3	VGLL3	ISLR	VGLL3	ADAMTS2	COMP	ADAMTS2	LOX	MFAP2	LOXL1	MMP11	MMP11	SRPX2	ASPN	COL6A3	TNFSF4	VDR	RUNX2	SMC4	TOP2A	THY1	TTC12
TNFAIP6	COPZ2	FN1	CDH11	COL12A1	MMP2	ISLR	THY1	HNT	CDH11	SFRP4	IGHG1	GAS1	LGALS1	PCOLCE	PPAPDC1A	KIAA1199	MFAP2	HGD	CDCA8	FN1	C13orf34
COPZ2	OLFML2B	TWIST1	ARL4C	C1QTNF6	TSHR	AEBP1	ITGBL1	COL16A1	RUNX2	GLT8D2	VCAN	DPYSL3	THY1	OLFML2B	AEBP1	COL8A1	GJB2	BIRC5	DPY19L2	SFRP2	CCRL2
EDNRA	ITGBL1	OLR1	HOPX	C16orf89	MAOA	MMP11	POSTN	MFAP5	LUM	RCN3	MMP2	TNFAIP6	CTSK	MFAP5	MFAP5	MFAP5	IL1RN	HNT	SLC20A1	ADAMTS2	MKI67
LPPR4	PLAU	COL6A3	COL6A3	BCAT1	ID4	C1QTNF6	MRC2	ADAM12	ITGBL1	WISP1	ASPN	PLAU	TNFAIP6	PPAPDC1A	ITGA11	LOC401097	GLT8D2	COL12A1	SMC4	SPARC	ACADL

NOTE: The overlapping genes have been indicated with different colors.

*Gene	**Weighted Averaged MI
COL11A1	0.850
COL10A1	0.468
THBS2	0.402
COL5A2	0.396
COL1A1	0.390
INHBA	0.387
FAP	0.373
COL5A1	0.371
COL1A2	0.349
POSTN	0.339
ADAM12	0.331

* An aggregate list of genes ranked in terms of a weighted average of the mutual information with *COL11A1*.

**the mutual information was weighted by the sample size of each data set.

Table 4: Top ranked (multiple-test corrected $P < 10^{-16}$) differentially expressed miRNAs in MAF signature in the TCGA ovarian cancer data set in terms of their association with *COL11A1*.

miRNA	**MI**	**Up/Down Regulated**
hsa-miR-22	0.204	*Up*
hsa-miR-514-1|hsa-miR-514-2|hsa-miR-514-3	0.193	*Down*
hsa-miR-152	0.187	*Up*
hsa-miR-508	0.168	*Down*
hsa-miR-509-1|hsa-miR-509-2|hsa-miR-509-3	0.164	*Down*
hsa-miR-507	0.152	*Down*
hsa-miR-509-1|hsa-miR-509-2	0.147	*Down*
hsa-miR-506	0.146	*Down*
hsa-miR-509-3	0.144	*Down*
hsa-miR-214	0.128	*Up*
hsa-miR-510	0.116	*Down*
hsa-miR-199a-1|hsa-miR-199a-2	0.115	*Up*
hsa-miR-21	0.112	*Up*
hsa-miR-513c	0.108	*Down*
hsa-miR-199b	0.103	*Up*

Table 5: Top ranked (multiple-test corrected $P < 10^{-16}$) differentially methylated genes in MAF signature in the TCGA ovarian cancer data set in terms of their association with *COL11A1*.

Methylation site	MI	Hyper-/Hypomethylated
PRAME	0.223	*Hyper*
SNAI1	0.183	*Hyper*
KRT7	0.158	*Hyper*
RASSF5	0.157	*Hyper*
FLJ14816	0.155	*Hyper*
PPL	0.155	*Hyper*
CXCR6	0.153	*Hypo*
SLC12A8	0.148	*Hyper*
NFATC2	0.148	*Hyper*
HOM-TES-103	0.147	*Hypo*
ZNF556	0.147	*Hyper*
OCIAD2	0.146	*Hyper*
APS	0.142	*Hyper*
MGC9712	0.139	*Hyper*
SLC1A2	0.136	*Hyper*
HAK	0.131	*Hypo*
C3orf18	0.130	*Hyper*
GMPR	0.130	*Hyper*
CORO6	0.128	*Hyper*

Table 6: Data sets that were used in the paper

Data set name	Source Site	GEO Accession	Affymetrix platform	Sample size
TCGA ovarian cancer	The Cancer Genome Atlas		HT_HG-U133A[a]	377
CCR ovarian cancer	Gene Expression Omnibus	GSE9891	HG-U133_Plus_2[b]	285
CCR colon cancer	Gene Expression Omnibus	GSE14333	HG-U133_Plus_2	290
Moffitt colon cancer	Gene Expression Omnibus	GSE17536	HG-U133_Plus_2	177
Singapore gastric cancer	Gene Expression Omnibus	GSE15459	HG-U133_Plus_2	200
Yu multicancer tumor	Gene Expression Omnibus	GSE5364	HG-U133A[c]	270 [341][d]
expO batch 1	Gene Expression Omnibus	GSE2109	HG-U133_Plus_2	60
expO batch 2	Gene Expression Omnibus	GSE2109	HG-U133_Plus_2	163
expO batch 3	Gene Expression Omnibus	GSE2109	HG-U133_Plus_2	164
expO batch 4	Gene Expression Omnibus	GSE2109	HG-U133_Plus_2	163
expO batch 5	Gene Expression Omnibus	GSE2109	HG-U133_Plus_2	160
expO batch 6	Gene Expression Omnibus	GSE2109	HG-U133_Plus_2	160
expO batch 7	Gene Expression Omnibus	GSE2109	HG-U133_Plus_2	156
expO batch 8	Gene Expression Omnibus	GSE2109	HG-U133_Plus_2	160
expO batch 9	Gene Expression Omnibus	GSE2109	HG-U133_Plus_2	240
expO batch 10	Gene Expression Omnibus	GSE2109	HG-U133_Plus_2	180
expO batch 11	Gene Expression Omnibus	GSE2109	HG-U133_Plus_2	180
expO batch 12	Gene Expression Omnibus	GSE2109	HG-U133_Plus_2	125
expO batch 13	Gene Expression Omnibus	GSE2109	HG-U133_Plus_2	62
expO batch 14	Gene Expression Omnibus	GSE2109	HG-U133_Plus_2	62
expO batch 15	Gene Expression Omnibus	GSE2109	HG-U133_Plus_2	60
expO batch 16	Gene Expression Omnibus	GSE2109	HG-U133_Plus_2	63

[a]Affymetrix HT Human Genome U133A Array
[b]Affymetrix Human Genome U133 Plus 2.0
[c]Affymetrix Human Genome U133A
[d]270 out of 341 samples are tumor samples.